Pramāṇa, Vol. 6 No. 5, 1976, pp. 305–311 © Printed in India.

Modification of Lytle's theory: Interpretation of the extended fine structure associated with L_{III} absorption discontinuity of some ytterbium systems

PRANAWA DESHMUKH, PRABODHACHANDRA DESHMUKH and CHINTAMANI MANDE
Department of Physics, Nagpur University, Nagpur 440010

MS received 20 October 1975; after revision 29 January 1976

Abstract. In Lytle's theory for the extended fine structure in x-ray absorption spectra, the potential at the boundary of the 'equivalent sphere' around the absorbing atom, having volume equal to that of the Wigner-Seitz cell is considered to be infinite. It has been observed that Lytle's theory is applicable only in the case of metals and metallic systems. In the present paper the extended fine structure associated with the L_{III} absorption spectra of some systems of ytterbium is interpreted on the basis of Lytle's model, modified by using a finite potential instead of an infinite one at the boundary of the equivalent sphere. The values of this potential are estimated for eight systems of ytterbium. It has been shown that there exists a correlation between the potentials and covalency of the compounds.

Keywords. Lytle's theory; extended fine structure; L_{III} absorption discontinuities covalency; rare-earths.

1. Introduction

Lytle's theory (Lytle 1964, 1966) offers a simple and convenient phenomenological interpretation of the extended fine structure (EFS) of x-ray absorption discontinuities. In this theory, the allowed energy states available to ejected photoelectrons in the x-ray absorption process are obtained by solving the Schrödinger equation,

$$\nabla^2 \psi + \frac{2m}{\hbar^2}[E - V(r)]\psi(r) = 0 \tag{1}$$

where the potential $V(r)$ is chosen such that

$$V(r) = 0 \quad \text{for} \quad r < r_s \tag{2a}$$

and

$$V(r) = \infty \text{ for } \quad r > r_s. \tag{2b}$$

Lytle has obtained the following relation between E and Q,

$$E = \frac{h^2}{8mr_s^2} Q\,, \tag{3}$$

roots of the half-order Bessel function appearing in the radial part of the wave

where E refers to the energy of the absorption maxima in the EFS, Q to the zero-equation and r_s is the radius of a sphere surrounding the absorbing atom having volume equal to that of the Wigner-Seitz cell. According to equation (3), the (E, Q) plots are linear and should pass through the origin. However, it has been observed (Chivate *et al.* 1968; Deshmukh and Mande, 1974; Kondawar and Mande, 1976) that while the (E, Q) plots pass almost through the origin for pure metals as well as for systems which possess metallic properties, they do not do so for non-metallic compounds. Chivate *et al* have proposed a model based on Lytle's theory for the EFS associated with the K absorption edges. In this model, they have used at r_s a finite potential instead of the infinite potential assumed in the original theory. In the present paper we show how this model can be used to explain the EFS corresponding to initial levels with different symmetries. As an illustration of this method, we have applied the model to the x-ray L_{III} absorption spectrum of ytterbium in the metal and in several of its compounds.

2. The Generalised model

The fact that the (E, Q) plots for compounds do not pass through the origin necessitates a reconsideration of the infinite-potential-approximation in Lytle's theory. Employing a finite potential at $r = r_s$, it has been shown by Chivate *et al* (1968) that applying the usual boundary conditions for the continuity of the wave function and its derivative at $r = r_s$, one gets,

$$\frac{\alpha}{j_l(\xi)} \frac{d}{d\xi} [j_l(\xi)] = \frac{\beta}{h_l^{(1)}(i\eta)} \frac{d}{d\eta} [h_l^{(1)}(i\eta)], \tag{4}$$

where

$$j_l(\xi) = \left(\frac{\pi}{2\xi}\right)^{1/2} J_{l+1/2}(\xi).$$

J is an ordinary Bessel function of half odd integer order, $h_l(i\eta)$ the spherical Henke function, and ξ and η are respectively equal to αr_s and βr_s.

The above equation is a generalised relation incorporating the symmetry of the initial levels and can be applied to electronic transitions to levels of appropriate symmetries.

In $L_{II, III}$ absorption spectra the initial level has p symmetry and therefore consideration of the electric dipole ($p \rightarrow d$) transitions reduces equation (4) to the following form:

$$\frac{\xi(9 - \xi^2)\cos\xi + (4\xi^2 - 9)\sin\xi}{3\xi\cos\xi - (3 - \xi^2)\sin\xi} = \frac{\eta^3 + 4\eta^2 + 9\eta + 9}{\eta^2 + 3\eta + 3}. \tag{5}$$

Squaring and adding ξ and η we get

$$\xi^2 + \eta^2 = \frac{2mV_0 r_s^2}{\hbar^2}. \tag{6}$$

The energy eigenvalues E are then given by

$$E = \frac{h^2}{8mr_s^2} Q', \tag{7}$$

where

$$Q' = \frac{\xi^2}{\pi^2} .$$

Equation (7) in the present model corresponds to equation (3) given by Lytle in his original theory. The (E, Q') plots will be linear and will pass through the origin provided that the values of Q' are consistent with eq. (5) and (6).

We observe that a parametric variation of the potential consistent with the above formalism gives rise to different sets of Q' values. Out of these sets one can choose an appropriate set leading to the best fit for the compounds. The inclusion of such adjustable parameters in the present model is guided by the principles of self-consistency, and is similar to the parametric representation of the APW muffin-tin potentials employed for certain band structure calculations (Freeman *et al.*, 1966).

The problem is now that of determining the values for Q' from those values of ξ which simultaneously satisfy the non-linear equations (5) and (6). The calculations were made on a CDC–3600 computer using the PROGRAM FINPOTEL developed by us for this purpose. A portion of the results of these calculations are presented in table 1 *a* which gives the values of Q' used in the present work. Each row of Q' values in this table corresponds to a potential given by:

$$V_0 = \frac{\hbar^2 \pi^2}{2m} \times \frac{J^2}{r_s^2} \text{ ergs}, \tag{8}$$

where J is the radius of the circle (eq. 6) in units of π. In table 1 (*b*) are given for the sake of comparison Lytle's values of Q for $l = 2$ ($p \rightarrow d$ transitions).

3. Comparison with experiments

The prominent absorption peaks in the EFS on the high energy side of the L_{III} absorption discontinuity of ytterbium reported by us earlier (Deshmukh and Mande,

Table 1 *a*.

J	Q'_1	Q'_2	Q'_3	Q'_4	Q'_5	Q'_6	Q'_7	Q'_8	Q'_9
5	3·05	7·46	13·39	21·70					
6	3·0.	7·53	13·76	21·97	27·85				
7	3·099	7·65	14·01	22·14	31·91	43·19			
8	3·10	7·75	14·18	22·45	32·48	44·14	53·61		
9	3·13	7·78	14·30	22·66	32·7	44·03	58·34	73·38	
10	3·15	7·87	14·43	22·9	33·12	45·18	59·02	74·22	91·51

Table 1 *b*. Lytle's values of Q for $l = 2$ ($p \rightarrow d$ transitions)

3·37	8·40	15·4	24·4	35 3	48 6	63·8	80·5	99·4

Table 2.

Sl. No.	System	Formula	Absorption maxima in EFS (in eV) A	B	C	D
1.	Yb-fluoride	YbF_3	8·2	46·8	103·2	174·8
2.	Yb-oxide	Yb_2O_3	8·2	46·8	107·4	179·0
3.	Yb-nitrate	$Yb(NO_3)\cdot 5H_2O$	9·4	44·3	100·7	166·2
4.	Yb-sulphate	$Yb_2(SO_4)_3\cdot 8H_2O$	9·4	45·9	95·7	157·8
5.	Yb-chloride	$YbCl_3\cdot 6H_2O$	9·0	44·3	97·7	157·8
6.	Yb-oxalate	$Yb(C_2O_4)_3\cdot 10H_2O$	9·0	43·5	93·2	149·3
7.	Yb-bromide	$YbBr_3\cdot 6H_2O$	9·4	45·1	94·8	153·5
8.	Yb-acetate	$Yb(CH_3COO)_3\cdot 6H_2O$	9·0	43·5	98·2	160·3
9.	Yb-metal*	Yb	9·8	26·2	49·1	7·56

* Yb-metal → E (113·9), F (157·6), G (206·8).

1974) are re-listed in table 2 for ytterbium metal and the following eight systems to facilitate discussion:

Ytterbium fluoride [YbF_3], ytterbium oxide [Yb_2O_3], ytterbium sulphate [$Yb_2(SO_4)_3\cdot 8H_2O$], ytterbium chloride [$YbCl_3\cdot 6H_2O$], ytterbium oxalate [$Yb(C_2O_4)_3\cdot 10H_2O$], ytterbium bromide [$YbBr_3\cdot 6H_2O$], ytterbium acetate [$Yb(CH_3COO)_3\cdot 6H_2O$] and ytterbium nitrate [$Yb(NO_3)_3\cdot 5H_2O$].

Choosing the appropriate set of Q' values, the (E, Q') plots have been plotted and are given in figure 1. It may be noticed that the (E, Q') plots now pass very well through the origin as against the (E, Q) plots reported earlier. The values of r_s, the equivalent sphere radius, obtained from these plots are given in table 3 using the formula:

$$r_s(\text{in } A) = \left(\frac{37\cdot 6}{M}\right)^{1/2} \tag{9}$$

where M is the slope of the curves. The potentials V_0 were then calculated using eq. (8). The results of these calculations are reported in table 3. The error in the values of the potentials, as estimated graphically, is within 5%.

4. Potential heights and covalency

We observe from table 3 that while V_0 is minimum in the case of the fluoride, it is maximum in the case of the acetate. This has led us to the consideration of the electronegativities of the bonding atoms (or groups of atoms). We observe that as the electronegativity of the bonding species decreases the height of the potential rises monotonically.

The ionicity I in a compound is given by (Philips, 1973)

$$I = 1 - \frac{v}{N}\exp(-\Delta\chi^2/4) \tag{10}$$

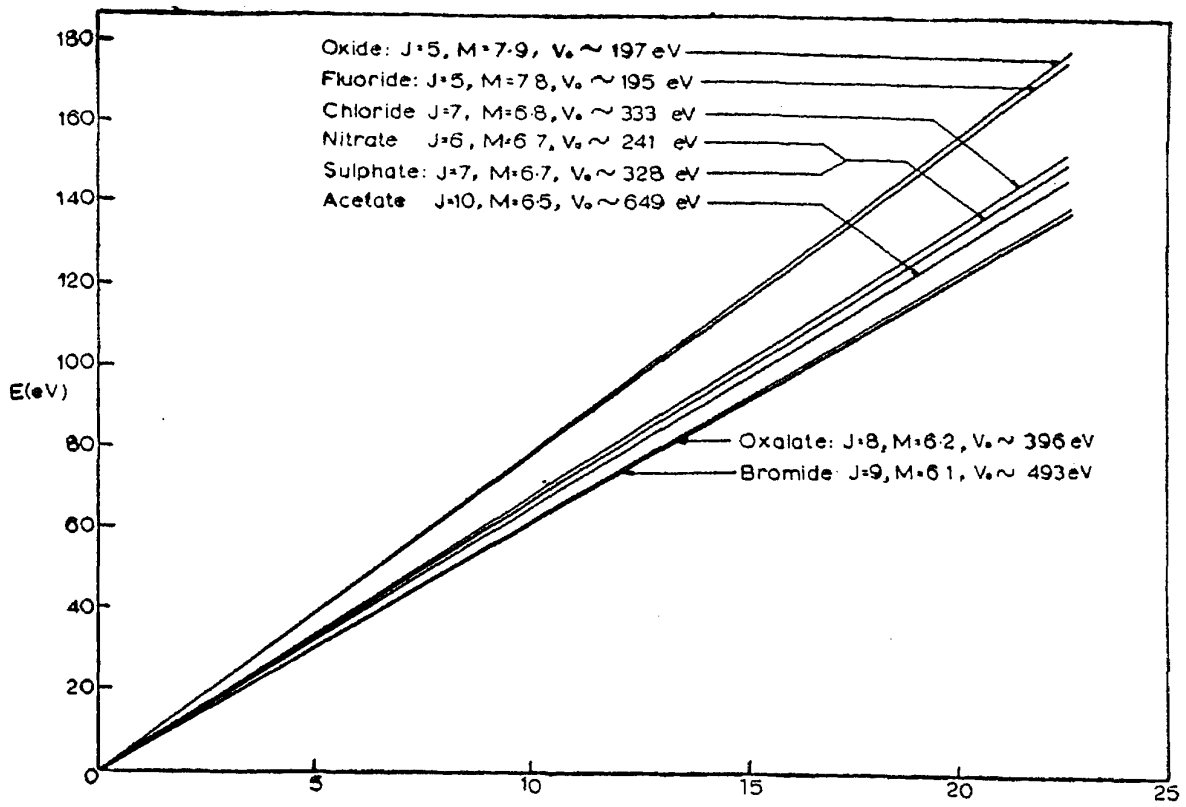

Figure 1. The E vs Q' plots. Obtained on using a finite potential at r_s.

Table 3.

Sl. No.	System	J	M	r_s (A)	V_0 (eV)	Electronegativity	
1.	Yb-fluoride	5	7·8	2·20	195	F :	5·75*
2.	Yb-oxide	5	7·9	2·18	197	O :	5·21*
3.	Yb-nitrate	6	6·7	2·37	241	NO_3 :	5·02**
4.	Yb-sulphate	7	6·7	2·37	328	SO_4 :	4·97**
5.	Yb-chloride	7	6·8	2·35	333	Cl :	4·93*
6.	Yb-oxalate	8	6·2	2·46	396	C_2O_4 :	4·69**
7.	Yb-bromide	9	6·1	2·48	493	Br :	4·53*
8.	Yb-acetate	10	6·5	2·40	649	CH_3COO :	4·04**
						Yb :	0·99*

* Value from Sanderson calculated on relative compactness scale (1967).

** Calculated by the authors using the concept of electronegativity equalisation.

where v is the valency, N the coordination number and $\triangle\chi$ the difference in the electronegativities of the bonding species. Therefore

$$\log_e \frac{CN}{v} = -0{\cdot}25\,(\triangle\chi)^2 \tag{11}$$

where C is the covalency of the compound given by $1 - I$. In figure 2 we have plotted a graph between $(\log_e V_0)$ and $(\triangle\chi)^2$. The slope of this plot which is a straight line is found to be $-0{\cdot}12$ and the intercept it makes on the $(\log_e V_0)$ axis is 7·6. Hence, the equation to this plot is:

$$\log_e V_0 = -0{\cdot}12\,(\triangle\chi)^2 + 7{\cdot}6 \tag{12}$$

eliminating $(\triangle\chi)^2$ between equations (11) and (12), we get

$$V_0 = KC^n \tag{13}$$

where $n \sim 0{\cdot}5$ in the present case.

We see that n depends on the relative slopes of the experimental $(\log_e V_0)$ vs. $(\triangle\chi)^2$ plots and the slope 0·25 that appears in eq. (11). It can be envisaged that the factors K and n in eq. (13) will depend upon the absorbing atom, symmetry of the initial level in which absorption takes place and the coordination number and valency of absorbing atom in a compound. Eq. (13) thus establishes a semi-empirical relationship between the potential V_0 and covalency, showing that as covalency rises the potential increases. In metals and in compounds having metallic properties, in which covalency is very high, the potential will tend to be of a very high order, as assumed in Lytle's original theory.

5. Conclusions

Our work suggests that while Lytle's approximation of an infinite potential barrier is well-suited for metallic systems, a parametric variation of the potential to a finite

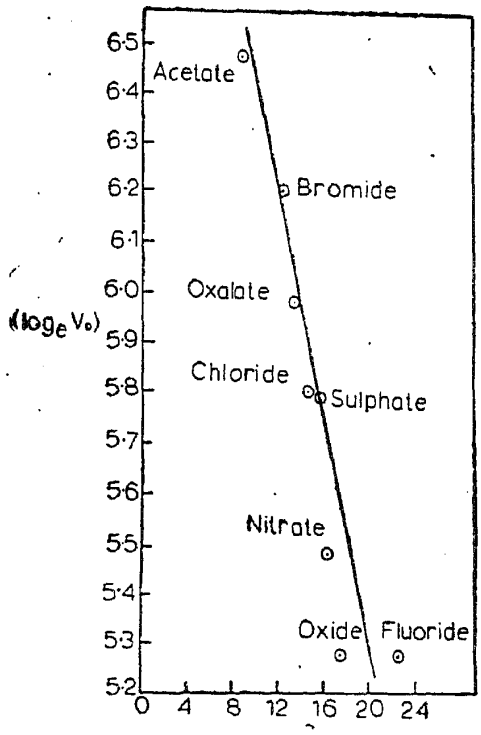

Figure 2. The relation between V_0 and $(\triangle\chi)^2$ for ytterbium compounds

height leads to more consistent results for ionic and ionocovalent compounds. The potential height, which appears to be a characteristic property of a system, is inversely related to the ionicity of the chemical bond. We may mention here that recent studies on the K absorption edges of some transition elements of the first series in their compounds have also shown that the applicability of Lytle's theory improves in systems of high metallicity (Chivate *et al.*, 1968; Kondawar and Mande, 1976).

It is difficult to assign a definite physical significance to the potential employed in the present model. The hole left behind in the atom and the immediate chemical environment of the abosorbing atom together determine the energy states in which the photoelectron can be trapped. The probabilities of the transitions are influenced by the symmetry of the initial and final states. Although the potential envisaged in obtaining the energy states has a transient existence during the x-ray absorption process, it appears to be determined by the covalency of the compound. It exists during the life-time of the hole state after which the various relaxation effects (Best, 1974) restore the equilibrium conditions, which may finally establish the static crystal potential. Further work is in progress and it is hoped that it will be possible to give a physical basis for the observed correlation between V_0 and covalency.

Acknowledgements

We are thankful to the TIFR, Bombay, for allowing us to make use of their computer facility. We are thankful to S. S. Kulkarni for his assistance. One of us (Pranawa Deshmukh) is thankful to the University Grants Commission, New Delhi, for a research fellowship.

References

Best P E 1974 *X-ray Spectroscopy* ed L V Azaroff p. 1–25, McGraw-Hill
Chivate P, Damle P S, Joshi N V and Mande C 1968 *J. Phys. C.* (*Proc. Phys. Soc.*) Ser 2 **1** 1171
Deshmukh P and Mande C 1974: *Pramana* **2** 138
Freeman A J, Dimmock J O and Watson R E 1966 *Quantum Theory of Atoms, Molecules and the Solid State* ed. P Lowdin p. 361, Academic Press
Kondawar V K and Mande C 1976 *X-ray Spectrometry* (in Press)
Lytle F W, 1964 *Proc. Int. Conf. Phys.* Non-Crystalline Solids, Delft North-Holland. p. 12 ed. J A Prins
Lytle F W 1966: *Adv. X-ray Analysis* **9** p. 398, Plenum Press.
Phillips J C 1973 *Bonds and Bands in Semiconductors* p. 33 Academic Press
Sanderson R T 1967 *Inorganic Chemistry* p. 69, Reinhold Publishing Corporation